PHYSICAL OPTICS

Original article
DOI: https://doi.org/10.18721/JPM.18411

FORMATION FEATURES OF HOLOGRAPHIC STRUCTURES RECORDED IN A COUNTER-DIRECTIONAL OPTICAL SCHEME ON THE PHOTOEMULSION EXPOSED TO SHORT-WAVE UV RADIATION

S. N. Gulyaev[1]✉, *N. M. Ganzherli*[2], *D. A. Ilyushina*[1], *I. A. Maurer*[2]

[1] Peter the Great St. Petersburg Polytechnic University, St. Petersburg, Russia;

[2] Ioffe Institute, St. Petersburg, Russia

✉ SGulyaev@spbstu.ru

Abstract. The article presents an experimental proof that it is possible to implement relief-phase recording of holographic information using an optical registration scheme in counter-propagating beams. Previously, this was done only for positive photoresists having a sensitivity three orders of magnitude lower than that of silver-halide photographic emulsion with other advantages. It has been experimentally shown that the key operations of photochemical processing of silver halide photographic emulsions are short-wavelength UV irradiation of photographic plates with a mercury lamp ($\lambda < 250$ nm) and their subsequent short-term (10 s) etching in glacial acetic acid. The mechanisms of surface relief formation in different ranges of recorded spatial frequencies were analyzed, and significant positive differences in the properties of relief-phase structures on silver halide photographic emulsions were shown compared to their counterparts recorded on photoresist.

Keywords: counter-directional scheme, diffraction efficiency, silver halide photoemulsion, holographic grating, surface relief

Citation: Gulyaev S. N., Ganzherli N. M., Ilyushina D. A., Maurer I. A, Formation features of holographic structures recorded in a counter-directional optical scheme on the photoemulsion exposed to short-wave UV radiation, St. Petersburg State Polytechnical University Journal. Physics and Mathematics. 18 (4) (2025) 151–166. DOI: https://doi.org/10.18721/JPM.18411

Научная статья
УДК 535.412; 532-3
DOI: https://doi.org/10.18721/JPM.18411

ОСОБЕННОСТИ ФОРМИРОВАНИЯ ГОЛОГРАФИЧЕСКИХ СТРУКТУР, ЗАПИСАННЫХ В КОНТРНАПРАВЛЕННОЙ ОПТИЧЕСКОЙ СХЕМЕ НА ФОТОЭМУЛЬСИИ, ПОДВЕРГНУТОЙ УФ-ОБЛУЧЕНИЮ

С. Н. Гуляев[1]✉, *Н. М. Ганжерли*[2], *Д. А. Ильюшина*[1], *И. А. Маурер*[2]

[1] Санкт-Петербургский политехнический университет Петра Великого, Санкт-Петербург, Россия;

[2] Физико-технический институт им. А. Ф. Иоффе РАН, Санкт-Петербург, Россия

✉ SGulyaev@spbstu.ru

Аннотация. В статье представлено экспериментальное доказательство возможности реализовать рельефно-фазовую запись голографической информации с помощью оптической схемы регистрации во встречных пучках. Ранее это было сделано только для позитивных фоторезистов, имеющих чувствительность на три порядка ниже, чем у галоидосеребряной фотоэмульсии, обладающей над ними и другими преимуществами. Экспериментально показано, что ключевыми операциями фотохимической обработки галоидосеребряных фотоэмульсий являются коротковолновое УФ-облучение фотопластинок ртутной лампой ($\lambda < 250$ нм) и их последующее кратковременное (10 с) травление в ледяной уксусной кислоте. Проанализированы механизмы формирования поверхностного рельефа в разных диапазонах регистрируемых пространственных частот и показаны существенные позитивные отличия свойств рельефно-фазовых структур на галоидосеребряных фотоэмульсиях от аналогов, записанных на фоторезисте.

Ключевые слова: контрнаправленная схема, дифракционная эффективность, галоидосеребряная фотоэмульсия, голографическая решетка, коротковолновое УФ-излучение, поверхностный рельеф

Ссылка для цитирования: Гуляев С. Н., Ганжерли Н. М., Ильюшина Д. А., Маурер И. А. Особенности формирования голографических структур, записанных в контрнаправленной оптической схеме на фотоэмульсии, подвергнутой УФ-облучению // Научно-технические ведомости СПбГПУ. Физико-математические науки. 2025. Т. 18. № 4. С. 151–166. DOI: https://doi.org/10.18721/JPM.18411

Introduction

A holographic recording setup with counter propagating beams (counter-directional scheme) was proposed by Yuri Denisyuk in 1962 [1]. This recording setup is widely used in visual holography to obtain three-dimensional images of real objects. The holographic structures (HSs) obtained by this method are reflective. In the case of plane object and reference beams, they represent a set of parallel planes (traces) corresponding to periodic modulation of the refractive index within the photosensitive medium (Fig. 1,*a*).

The period of the internal HS d_{int} weakly depends on the angles of incidence of the reference and object beams on the recording medium and is approximately equal to half the wavelength λ of light in a photosensitive medium $d_{int} = \lambda/2n_0$ (n_0 is the average refractive index of the photosensitive medium). Since the traces of the internal structure emerge onto the surface at an oblique angle (see Fig. 1,*a*), the period of the HS on the surface of the photosensitive medium d_{surf} differs significantly in magnitude from the period of the internal structure d_{int}. For example, the laser (object) beam is reversed relative to the incident (reference) beam in the setup with counter

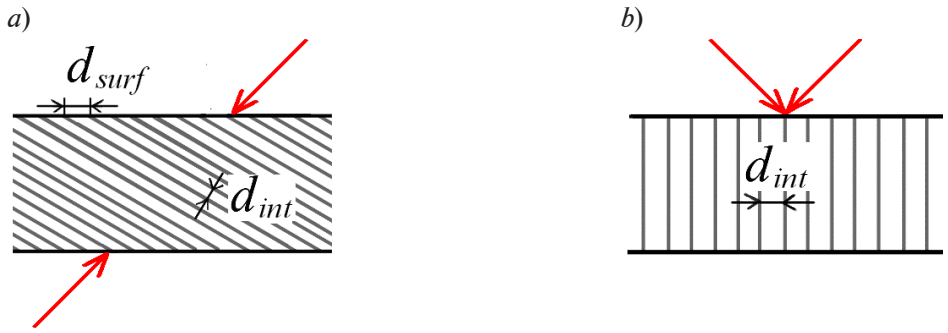

Fig. 1. Optical setups for recording three-dimensional images of an object: with counter propagating (*a*) and converging (*b*) laser beams; d_{int}, d_{surf} are the periods of the internal holographic structure (HS) and HS on its surface, respectively

propagating beams in Fig. 2,*a*. In this case, the spatial period of the grating on the surface can be widely varied by changing the inclination of the grating traces within the photographic material by the formula

$$d_{surf} = \lambda/(2\cos\theta_0). \quad (1)$$

The spatial frequency of the HS on the surface is $\nu_{surf} = 1/d_{surf}$, varying in the range from 0 to 3175 mm^{-1} (Fig. 2,*b*) depending on the rotation angle θ_0 of the photographic plate placed in front of the mirror (Fig. 2,*a*). The graph in Fig. 2,*b* corresponds to the case when a helium-neon laser with a wavelength $\lambda = 0.63$ μm is used for holographic recording.

The surface period cannot be realized in the idealized HS recorded in the setup with counter

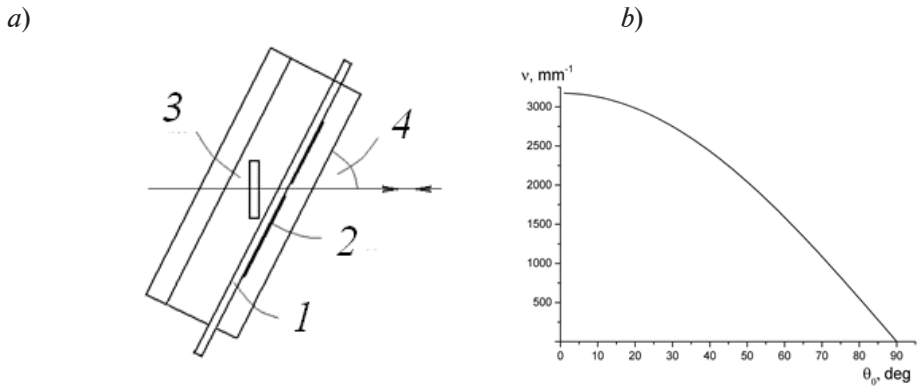

Fig. 2. Variation of surface spatial frequency ν: setup with counter propagating beams (*a*); dependence of this frequency on the rotation angle of the photographic plate θ_0 (*b*) photographic plate *1*; aperture *2*, mirror *3*, rotation angle 4 of photographic plate

propagating beams (Fig. 3,*a*), so that the entire structure is a pure volume grating, operating in reflection. However, in real experiments using silver halide photoemulsion (SHP), the internal trace structure of the recorded silver (Ag-) image often becomes distorted near the surface (Fig. 3,*b*). These distortions can give rise to a surface grating whose optical properties differ significantly from the diffraction properties of the internal volume grating. The surface grating may form because the grating traces change shape as photochemical processing is non-uniform over the thickness of the SHP layer. A periodic surface relief (Fig. 3,*c*) may also serve as an additional factor contributing to the formation of the surface HS. This relief is influenced by the physical volume occupied by the silver grains in the developed photographic material as well as the varying degree of hardening (cross-linking) of the gelatin surface layer [2]. The surface relief can also be produced forcibly, by selective exposure of the gelatin in the photosensitive layer, for example, to short-wave ultraviolet radiation [3].

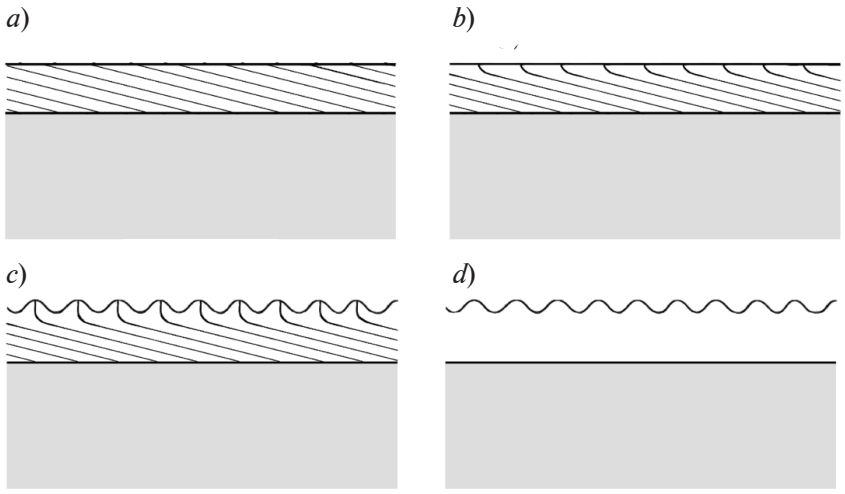

Fig. 3. Surface HS for silver halide emulsion: idealized holographic structure (*a*); distortion of the internal Ag-image traces near the surface of the photosensitive medium (*b*); formation of periodic surface relief (*c*); holographic spatially periodic structure with high efficiency and low angular selectivity (*d*)

It is especially important to be able to purposefully form a surface structure as a relief in experimental conditions, while simultaneously eliminating the internal absorption grating, since this makes it possible to obtain holographic spatially periodic structures with high efficiency and low angular selectivity, which is in demand for various technological applications in optics (Fig. 3,*d*). Such a technique was first implemented in [4], where thin layers of positive photoresist were used. In such a photosensitive material, the regions most illuminated by visible light are degraded during the development process and dissolve in the etchant (see Fig. 4,*a*). The traces of the internal grating shown in Fig. 4,*a* correspond to the nodal planes with the lowest intensity for the photoresist exposed to coherent light from a 488 nm argon laser. The distance h from the end of one of the traces of the internal structure coming to the surface to the nearest trace located below along the normal to the surface practically does not change when the surface spatial frequency is varied. This parameter determines the maximum etching depth h_{etch}. This depth, amounting to about 0.22 μm (Fig. 4,*b*) for a relief with a sawtooth profile after surface metallization, turns out to be sufficient for forming highly efficient blazed reflective gratings, which are still widely used in spectroscopy [5].

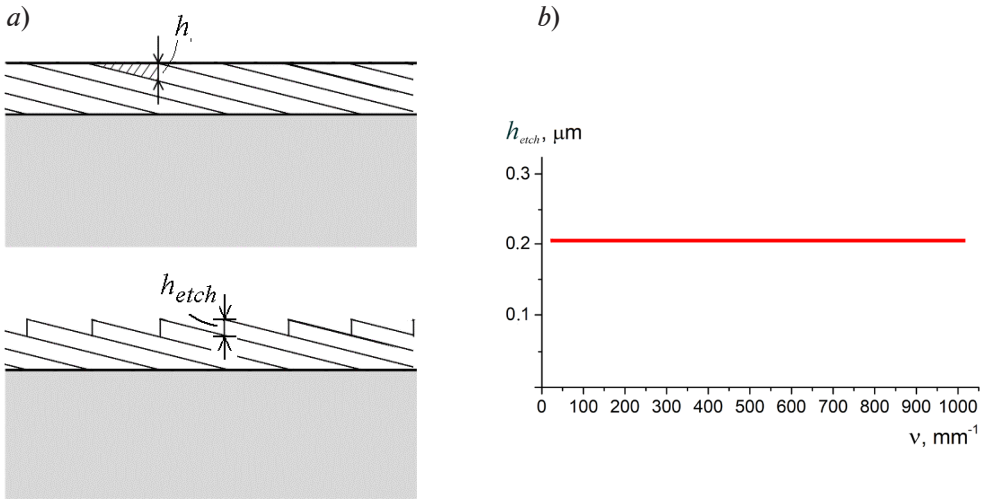

Fig. 4. Influence of etching positive photoresist on its properties: formation of relief-phase surface structure (*a*); dependence of etching depth h_{etch} on the surface spatial frequency ν (*b*)

Goals and objectives

Gelatin-containing photosensitive media such as silver halide photoemulsion and dichromated gelatin are widely used in holography. Exposure to short-wave UV radiation (λ = 315–400 nm) produces various surface and volume HS on these media combined with dichromates, due to cross-linking of gelatin macromolecules (see [6] as an example). As the wavelength decreases ($\lambda \leq$ 250–270 nm), the mechanism of the transformations induced by UV radiation is reversed. Absorption of high-energy photons induces the breaking of chemical bonds in the main chains of gelatin macromolecules (photolysis, photodegradation) in the absence of any added sensitizers, including dichromates. Methods for forming the surface relief in gelatin-containing photosensitive media via the recording setup with converging beams (see Fig. 1,*b*) were developed based on the effect of short-wave UV radiation on gelatin and subsequent etching of its regions subjected to the greatest photolysis [7].

The main stages of photochemical processing responsible for forming surface relief are as follows.

At the *first stage*, after exposure of the photographic plate, a primary HS is produced by standard photographic development and fixation, appearing as a black-and-white Ag image of interference traces.

The second stage is aimed at selective tanning of the photoemulsion layer, concentrated in regions with the highest Ag-image density. This is accomplished using dichromate-based tanning bleaches. Subsequent fixation in a solution of sodium thiosulfate ($Na_2S_2O_3$) makes it possible to completely remove the Ag image from the photoemulsion layer. Thus, an HS is created after the second main stage of photochemical processing; the degree of gelatin tanning in this HS varies periodically in accordance with the recorded interference pattern. This structure effectively modulates the photodegradation of gelatin in the plates exposed to short-wave UV radiation from a mercury-quartz lamp. The more tanned (i.e., hardened or cross-linked) regions are more resistant to the degrading effect from high-energy UV radiation at wavelengths below 250 nm due to a large number of cross-links between gelatin macromolecules. Therefore, adjacent, less hardened regions with fragmented gelatin macromolecules are easily dissolved in a suitable solvent such as water or glacial acetic acid (CH_3COOH) at the third (main) stage of processing [7]. Thus, etching produces a deep relief with crests coinciding with the most hardened (tanned) regions and forming a highly efficient transmission-type relief-phase HS.

In contrast to photoresists, whose treatment after exposure to coherent light is limited only to etching with minimal swelling of the layer, photochemical treatment of SHP includes the first two main stages, where the photo layer is immersed in aqueous solutions and experiences very strong swelling.

However, methods [7] are used at the *third (main) processing stage* to minimize the degree of swelling in the gelatin layer. This is achieved, firstly, by using GAA as an etchant instead of water, and, secondly, by reducing the etching time to 10 seconds. Therefore, the method for processing SHP described above [7] is somewhat similar to the methods for processing positive photoresists [8]. On the other hand, the photosensitivity of SHP exceeds the photosensitivity of photoresists by almost a 1000 times, making it convenient to use these photographic materials in holography.

In view of the above, there is an interest in studying whether SHP can be used to record relief-phase HS not only in setups with converging beams but also with counter propagating beams. The preliminary results of such studies are presented in our works [9, 10].

Experimental procedure

The optical setup described above (see Fig. 2,*a*) was used to record the holographic gratings: the laser (object) beam reflected from the mirror is reversed with respect to the incident (reference) beam, and the spatial frequency of the grating is set by adjusting the rotation angle of the photographic plate θ_0, in accordance with the graph in Fig. 2,*b*. PFG-01 photographic plates were mainly used in the experiments; in some cases, PFG-03M plates were also used, which have a lower contrast of the primary silver image.

Table 1 outlines the main stages of the holographic process, detailing the complete photochemical treatment of the samples, the operations performed, equipment and reagents for implementing them.

Table 1

Holographic processing procedure of relief-phase gratings in the setup with counter propagating beams

Technological stage	Procedure	Equipment and reagents
I. Exposure of photographic plates to laser radiation	Latent Ag image of interference traces is generated (oblique planes of antinodes inside the SHP)	PFG-01 and PFG-03M photographic plates, He-Ne laser (10 mW)
II. Development of plates (4 min)	Primary holographic structure is formed as Ag image of interference traces	Kodak D-19 contrast developer
III. Fixation	Silver halides are removed from photosensitive layer	$Na_2S_2O_3$-based fixer
IV. Drying	SHP is dehydrated	Air environment
V. Tanning bleaching	Gelatin is selectively tanned in regions with highest density of Ag image (cross-links between macromolecules are created using Cr^{3+} ions)	R-10-type bleach with ammonium dichromate $(NH_4)_2Cr_2O_7$
VI. Fixation	Silver salts are removed from photosensitive layer	$Na_2S_2O_3$-based fixer
VII. Clearing	Coloring Cr compounds are removed from SHP layer. Gelatin tanning is completed	2% Na_2SO_3 solution
VIII. Drying	SHP is dehydrated	Air environment
IX. Short-wave UV irradiation (25 min)	Gelatin undergoes photodegradation in the least tanned regions of photosensitive layer	DRT-230 mercury lamp (230 W power)
X. Short-term etching (10 s)	Photodegraded regions of gelatin areas are etched away; surface-relief holographic structure is formed	CH_3COOH or CH_3COOH + isopropanol (C_3H_8O)
XI. Removal of CH_3COOH, drying	Gelatin etching is rapidly interrupted, residual reagents are removed from surface of photosensitive layer	Isopropanol (C_3H_8O) baths + air-stream drying

Thus, photochemical processing of photographic plates was ultimately aimed at initiating the surface grating while simultaneously eliminating the internal HS. The main parameter studied in the experiment was the diffraction efficiency (DE) of holographic gratings, defined as the ratio of the intensity of the +1 order diffracted beam to the intensity of the incident beam for a transmission-type grating at an optimal incidence angle. The wavelength of the readout beam was, the same as during the recording, 0.63 μm.

The DE value was measured after stages IV (DE of primary amplitude HS), VIII (DE of relief-phase hologram after selective tanning and removal of silver salts from the gelatin layer) and XI (DE of this hologram after UV irradiation and etching), see also Table 1. Optical density was also measured for samples with primary amplitude HSs (defined as the decimal logarithm of the ratio of the light intensity transmitted through the sample to the incident beam intensity).

The OPT101 monolithic photodiode (Texas Instruments) was used to measure the intensity of laser radiation. The profiles of the surface reliefs of the holographic gratings were studied using an MII-4 Linnik microinterferometer. The height (depth) of the surface relief h was determined as the difference between crests and valleys. The diffraction spectra of the samples were studied using far-field pattern photographs and by measuring the DE in different diffraction orders.

Diffraction efficiency of holographic structures and recording parameters. Measuring the DE samples of holographic gratings at different surface spatial frequencies, we detected certain characteristics of the photosensitive medium subjected to complex multistage processing. Fig. 5 shows the dependences of the obtained values of DE for the holographic gratings on the time t during which the photographic plates were exposed to laser light, for a wide range of spatial frequencies: 36–730 mm^{-1}. DE measurements were carried out at different stages of photochemical processing described in the previous section.

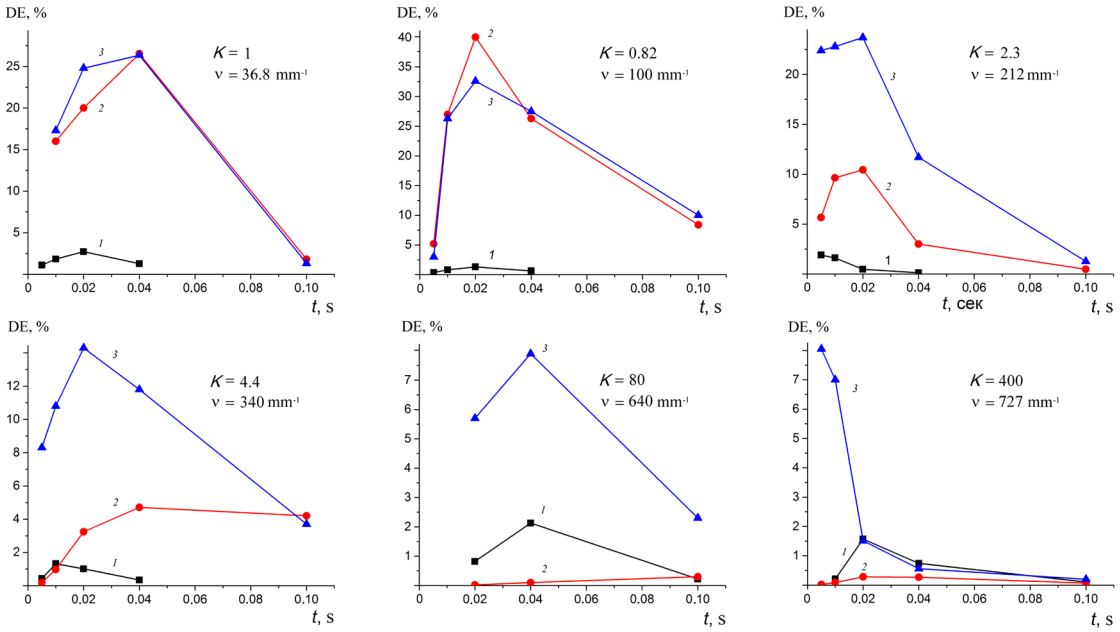

Fig. 5. Dependences of DE on exposure time t for holographic grating samples, in ascending order of surface spatial frequencies for PFG-01 plates at different processing stages (see Table 1): DE of primary amplitude hologram after stage IV *1*; DE of relief-phase hologram after stage VIII (removal of internal structure) *2*; DE of relief-phase hologram after complete processing (stage XI) *3*

As can be seen from Fig. 5, the maximum DE in primary amplitude HSs is approximately 2% (curves *1*). Therefore, the surface structure appears at the stage when the Ag image is formed, after development and fixation. In this case, the maximum DE is virtually independent of the spatial frequency, since PFG-01 has a high resolution for recording the amplitude Ag image, exceeding 1000 mm^{-1}.

The following observations can be made for the maximum DE of relief-phase holograms, measured before (curves *2*) and after (curves *3*) UV irradiation of samples from the mercury lamp and etching:

1) the maximum DE values of relief-phase holograms subjected to complete processing correspond to the average optical densities of the primary amplitude HS, lying in the range $D = 0.6–1.5$;

2) the maximum DE values for the samples not exposed and exposed to UV radiation and subsequent etching in GAA practically coincide in the region of relatively low spatial frequencies ($\nu < 100$ mm^{-1});

3) as the spatial frequency increases, the difference between the maximum DE values for dependences *2* and *3* in Fig. 5 increases rapidly in the region $\nu > 100$ mm^{-1}. On the other hand, the DE value for the non-irradiated samples tends to zero ($DE_{max} \le 0.2\%$ at $\nu > 727$ mm^{-1}), DE_{max} for the samples exposed to UV radiation and etched in GAA tends to $DE_{max} \approx 8\%$;

4) the latter circumstance can be characterized using the diffraction efficiency enhancement factor K, equal to the ratio of the maximum value of DE after exposure to UV radiation and etching in CH_3COOH to the value of DE before irradiation and etching at the same time of exposure to coherent radiation t. The K value for DE_{max} is shown in each graph in Fig. 5;

5) we detected a particular characteristic of the gratings recorded in the setup with counter propagating beams, distinguishing it from the similar procedure for gratings recorded in the setup

Table 2

Parameters of relief-phase holographic gratings depending on processing technology used for photoemulsion layers

ν, mm^{-1}	Concentration of CH_3COOH solution in C_3H_8O, %	DE_{max}, %	*K* value
566	25	0.65	3.8
550	50	0.47	6.7
551	50	0.74	2.1
551	50	1.13	2.2
566	100	5.20	403
639	100	7.90	285
727	100	8.05	> 402

Notations: ν is the recorded spatial frequency; DE_{max} is the maximum achieved value of diffraction efficiency, *K* is the enhancement factor of DE_{max}.

with converging beams. The feature is that recording HS on PFG-01 via the setup with converging beams yields significantly high values of the enhancement factor $K = 200–500$ at a spatial frequency $\nu = 1200$ mm^{-1} if a 50% CH_3COOH solution in isopropanol (C_3H_8O) is used as an etchant [9]. In contrast, samples that have undergone full processing in the recording setup with counter propagating beams at high spatial frequencies above 500 mm^{-1} yield significant values of DE and *K* only if GAA used as the etchant is not diluted by isopropanol. This is reflected in Table 2, where the values of DE_{max} and *K* are given depending on the concentration of the etchant solution of CH_3COOH in C_3H_8O.

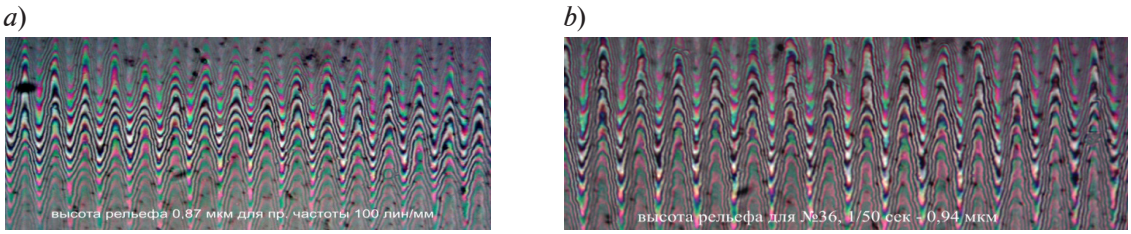

Fig. 6. Surface relief interferograms of the sample ($\nu = 100$ mm^{-1}): heights of spatial relief $h_{max} = 0.87$ μm (*a*) and 0.94 μm (*b*) before (*a*) and after (*b*) UV irradiation and etching, i.e., after stages VIII and XI (see Table 1)

Surface relief profiles and diffraction spectra of holographic structures. The angular dependences of DE provide significant information about the nature of HSs that underwent complete processing, including UV irradiation and etching. For example, for a sample with a spatial frequency of about 900 mm^{-1}, the full width at half maximum (FWHM) of the angular dependence of DE is approximately 40°, which, according to Kogelnik's theory, corresponds to a thickness of the diffracting structure of less than 1 μm. This value is a small fraction of the total thickness of PFG-01 photoemulsion, equal to 6-7 μm. Taking this into account, and because the internal structure was largely suppressed after Stage VI (see Table 1), we were justified in treating the resulting structures as pure-phase thin relief holograms (this was confirmed in further studies).

The MII-4 Linnik microinterferometer was used to obtain distinct surface relief profiles over the entire range of spatial frequencies researched. Importantly, the absolute values of the height of the spatial relief h_{max} increase sharply with a decrease in the spatial frequency below 150 mm^{-1}. UV irradiation and etching practically do not lead to an increase in the height of the surface relief (Fig. 6). Thus, the relief at low spatial frequencies is already formed after the wet processing stages are completed, and the contribution from the final stages of UV irradiation and etching is insignificant.

Large heights of the surface relief ($h_{max} \approx 1$ μm), achieved at low spatial frequencies ($\nu \leq 100$ mm^{-1}), are comparable to the depths of the surface relief obtained for pure-relief holograms recorded in the optical setup with converging beams [2, 3]. This sharply distinguishes the results achieved for SHP from those obtained for positive photoresists, whose h_{max} does not exceed 0.22 μm [4].

A sharp increase in the depth of the surface relief with a decrease in the spatial frequency of the recorded holographic gratings is confirmed by redistribution of light energy in diffraction spectra (diffraction orders). As the spatial frequency decreases, the intensities of the zero and first diffraction orders become equal around 212 mm^{-1} (Fig. 7,*a*).

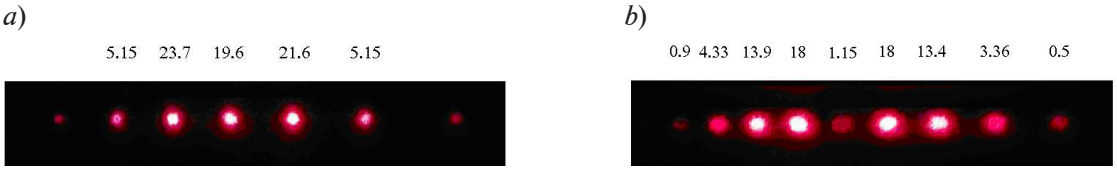

Fig. 7. Photographs of diffraction spectra for samples under normal incidence of illuminating laser beam, at spatial frequencies ν = 212 mm^{-1} (*a*) and 100 mm^{-1} (*b*). The numbers above the diffraction spots indicate the DE values (in %)

A further increase in the depth of the surface relief at relatively low spatial frequencies significantly reduces the fraction of non-scattered light (zero order) and leads to the transfer of light energy to higher diffraction orders (Fig. 7,*b*). The smallest fraction of the zero-order energy at a spatial frequency of 100 mm^{-1} is 1–3%.

Diffraction spectra for spatial frequencies of 100 and 212 mm^{-1} (Fig. 7), as well as interferograms (Fig. 6) show that the surface relief profiles in this region of spatial frequencies have a symmetric quasi-sinusoidal character. Experiments established that this is also true in the region of higher spatial frequencies. As an example, Fig. 8 shows an interferogram of the surface relief profile at a spatial frequency ν = 550 mm^{-1} for the PFG-03M photographic plate.

Fig. 8. Interferogram of relief profile for spatial frequency ν = 550 mm^{-1} (PFG-03M photographic plates)

Symmetrization of the surface relief profile in a wide range of spatial frequencies is a characteristic feature of SHP, distinguishing its properties from those of positive photoresists used to form asymmetric sawtooth-shaped reliefs during holographic recording in a setup with counter propagating beams. An asymmetric sawtooth-shaped relief profile was only detected in some samples at very low spatial frequencies, in the range of 30–40 mm^{-1} (Fig. 9,*a*), leading to an asymmetric distribution of light intensity in the diffraction spectrum (see Fig. 9,*b*).

The quasi-sinusoidal character of the surface relief profile in almost the entire spatial frequency domain is confirmed by direct calculations of DE using the procedures from the theory on thin holograms in the well-known Raman–Nath approximation. For example, for a relatively high spatial frequency of 550 mm^{-1} and the PFG-03M plates, the surface relief profiles can be measured in accordance with the interference pattern in Fig. 8. The relief heights h are markedly different for each specific point of the sample, therefore, this value was calculated based on the results of 8 measurements for adjacent crests and valleys. The obtained average relief depth h turned out to be 0.067 μm.

According to the theory of thin relief holograms, DE for the 1st diffraction order is described in the case of a sinusoidal relief by the following formula:

$$\eta = J_1^2\left(\frac{\pi h(n_0 - 1)}{\lambda}\right)\cdot 100\%, \qquad (2)$$

where J_1 is the first-order Bessel function of the first kind; λ is the laser radiation wavelength, λ = 0.63 μm; h is the height of the surface relief; n_0 is the average refractive index of gelatin, n_0 = 1.53.

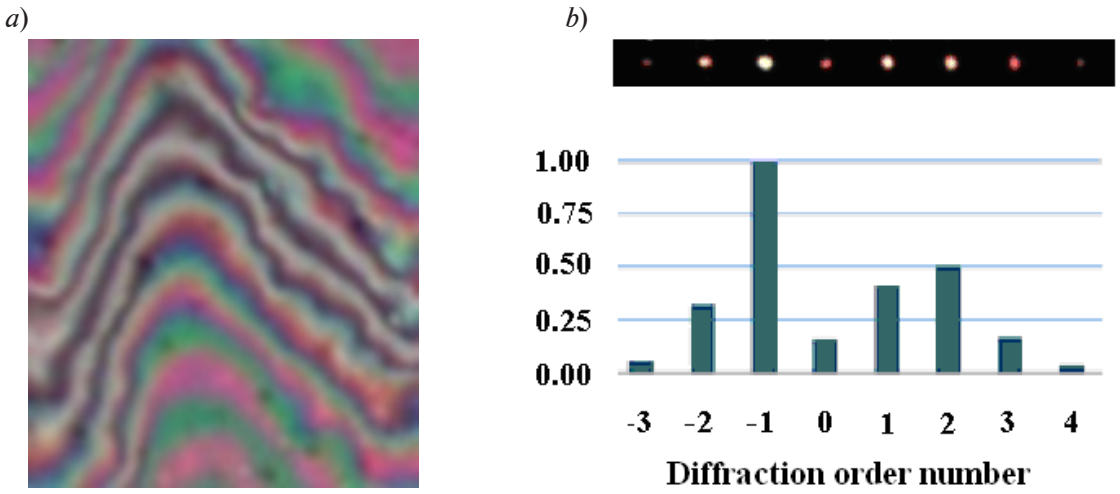

Fig. 9. Example of an interferogram of sawtooth-shaped relief profile for low spatial frequency (ν = 36.4 mm^{-1}) (*a*); photograph of diffraction spectrum with diffraction order numbers and distribution of relative light intensity among diffraction orders (*b*)

The DE calculated by Eq. (2) should be 0.78% for the relief height h = 0.067 μm. It follows, then, that the experimental DE values obtained in the range of 0.70–0.74%, as well as the corresponding calculated values, coincide with an accuracy of about 10%. We can conclude from here that the diffraction of light on the sample is due to the surface relief structure.

Similar results were obtained for the main PFG-01 plates used in this work and for a lower spatial frequency ν = 212 mm^{-1}, with relief heights increasing by more than 6 times compared to the previous case. This time, the values of h and DE were measured at three points of the sample: *A*, *B*, and *C*, located at significant distances from each other (Table 3).

Analyzing the data in Table 3, we can conclude that the experimentally measured DE values agree well with the theoretical ones calculated by Eq. (2).

As noted above, the maximum DE of PFG-01-based samples fully processed in the region of high spatial frequencies (over 500 mm^{-1}) tends to a value of about 8% (see Fig. 5). According to the theory on thin transmission-type holograms with a sinusoidal relief profile, the surface relief depth h can be calculated for this case using Eq. (2). In this case, the value $h \approx 0.22$ μm is obtained, which approximately coincides with the estimated maximum relief depth for a holographic recording setup with counter propagating beams using positive photoresists.

Therefore, the diffraction properties of HSs described in this section are adequately explained within the framework of the theory of thin holograms in the Raman–Nath approximation.

Table 3

Comparison of experimental and calculated DE values

Measuring point	h, μm	DE value, %	
		Experimental	Calculated (see Eq. (2))
A	0.42	22.43	19.9–23.7
B	0.46	25.21	
C	0.36	17.95	
Mean	0.41	21.86	

Spatial frequency responses and mechanisms of surface relief formation

The experimental data were used to construct the spatial frequency responses, reflecting the dependence of maximum DE before and after UV irradiation of the samples (Fig. 10,*a*) on the spatial frequency. Fig. 10,*b* shows similar dependences for the enhancement factor *K*. In this case, the *K* values are obtained by dividing the DE values for curve *2* by those for curve *1* (see Fig. 10,*a*).

Analyzing the data in Fig. 10,*a*, we find a significant difference in the spatial frequency

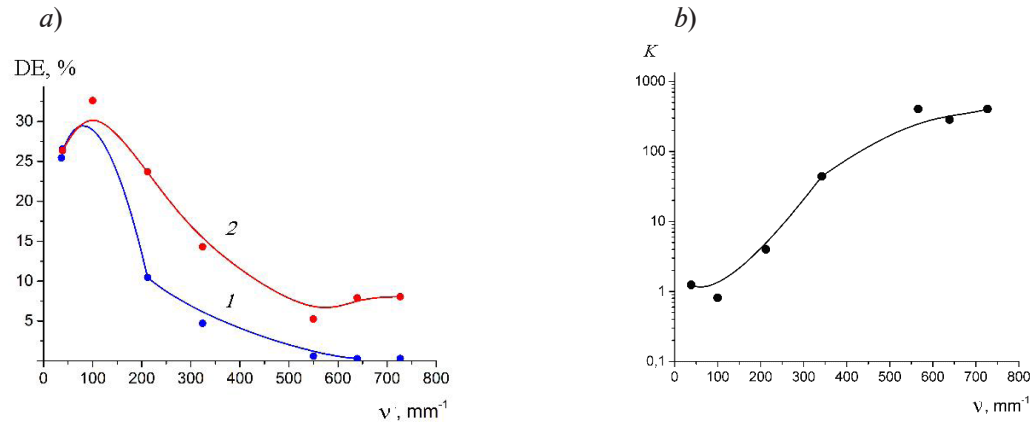

Fig. 10. Maximum DE of samples as function of spatial frequency ν after processing stages VIII (curve *1*) and XI (curve *2*) (see Table 1) (*a*); enhancement factor *K* as function of spatial frequency (*b*)

responses of relief-phase HSs whose DE was measured at different stages of photochemical processing. Samples that were not exposed to UV radiation and etching experience severe swelling in aqueous solutions at the water processing stages (see Stages I–VII, Table 1). This swelling eventually plays the decisive role in forming the surface relief during drying (see Stage VIII in Table 1).

The only mechanism responsible for high DE values and, consequently, large surface relief depths at relatively low spatial frequencies ($\nu < 150$ mm $^{-1}$) in these samples is, apparently, pulling of swollen gelatin volumes during drying of the wet colloid to the most tanned areas corresponding to the regions with the Ag image highest density in the primary amplitude hologram [2]. As in the case of the setup with converging beams [3], the mechanism of surface relief formation associated with the occurrence of tension forces in the drying colloid, provided large surface relief depths (about 1 μm) and a maximum DE equal to 30–40% for the setup with counter propagating beams. This result confirms the predictions of the theory on thin holograms for various shapes of surface relief at low spatial frequencies. The described mechanism is characterized by a rapid decrease in the spatial frequency response at spatial frequencies above 100 mm $^{-1}$, which is caused by the action of surface tension forces smoothing the surface relief [11]. According to [11], surface tension forces tend to minimize the surface area of the body. Therefore, an increase in the surface area of the dried photoemulsion layer with an increase in spatial frequency and a constant surface relief height is possible only until a certain threshold value ν_{thr} is reached. Given a sufficiently high spatial frequency, mechanical stresses introduced by surface tension overcome the bonding forces between gelatin molecules and can partially smooth the surface relief. Assuming that the area *S* of the surface HS remains constant at $\nu > \nu_{thr}$, we can calculate the height *h* of the surface relief at a given spatial frequency ν from the equation $S(\nu) = S(\nu_{thr})$, or otherwise from the equation

$$\nu \int_0^{1/\nu} \sqrt{1 + \pi^2 h^2 \nu^2 \cos^2 2\pi\nu x}\, dx = const, \qquad (3)$$

where *x* is the spatial coordinate on the surface of the photosensitive layer perpendicular to the grating traces.

Fig. 11,*a* compares the experimental spatial frequency response (see curve *1* in Fig. 10,*a*) with the theoretical one calculated based on the principles from [11]. As a first step, Eq. (2) was used to determine the relief height h for one of the points on the descending part of the experimental spatial frequency response. It was assumed that the profile shape of the surface relief was quasi-sinusoidal, in accordance with the calculations in the previous section. In particular, a point corresponding to a spatial frequency of 212 mm^{-1} was selected. Next, still assuming the profile shape of the surface relief to be sinusoidal, we calculated the relative surface area of the SHP layer, which is a constant (const) in Eq. (3). Further, if we perform calculations in reverse order in accordance with a brief scheme $S = \text{const} \rightarrow h \rightarrow J(...) \rightarrow \eta$, then we can obtain the calculated DE values for all spatial frequencies. The good agreement of the experimental spatial frequency response with the calculated one (see Fig. 11,*a*) confirms the hypothesis of relief formation due to forces arising during drying of wet swollen colloid gelatin.

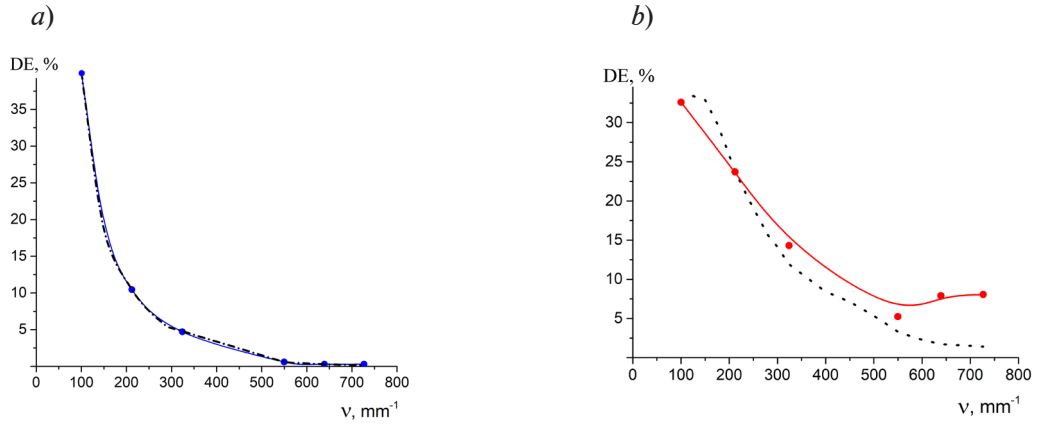

Fig. 11. Experimental (solid colored lines) and theoretical (dashed black lines) spatial frequency responses of DE for the samples at different stages: before UV irradiation and etching (*a*), after complete processing including these stages (*b*)

After the sample undergoes the final processing stages (UV irradiation and etching in GAA), the surface relief forms by a fundamentally different mechanism, associated with selective etching of photodegraded gelatin regions. First of all, this can be observed from the dependence of the enhancement factor K on the spatial frequency (see Fig. 10,*b*). It follows from this graph that the new mechanism governing relief formation begins to prevail over the previous one at frequencies above 200 mm^{-1}, reaching K values of the order of several hundred. The reason for the predominance of the new mechanism is that the harmful effect of surface tension forces smoothing the surface relief at high spatial frequencies was minimized. Special measures were taken for this purpose to reduce the degree of gelatin swelling at the stage of final processing (etching), in accordance with [12]. Glacial acetic acid was chosen as the solvent, causing less swelling of gelatin than water, while the etching time was reduced to 10 seconds. The theoretical framework developed to describe the spatial frequency responses of samples that did not undergo complete processing after UV irradiation and etching is inapplicable (see Fig. 11,*b*), since the theoretical curve deviates significantly from the experimental one, as it is calculated, as before, using Eq. (3) based on the initial spatial frequency of 212 mm^{-1}. The real spatial frequency responses of samples after complete processing extends much further into the region of high spatial frequencies.

Conclusion

A characteristic feature of the HS recorded in an optical setup with counter propagating beams is that traces (planes) of the internal grating appear on the surface at an oblique angle. Consequently, the etching depth $h_{etch} \approx 0.21-0.22$ μm for photoresists (see Fig. 4,*b*) does not depend on the recorded spatial frequency and the relief shape is sawtooth and asymmetric (see Fig. 4,*a*). Comparing silver halide photoemulsions (SHP) with photoresists, we can find both similarities and significant differences in the properties of holographic structures recorded in the setup with counter propagating beams. The differences consist both in the large discrepancy between

the thicknesses (SHP is about 7 μm, and the photoresist layers are less than 1 μm) and in the significantly greater susceptibility of SHP to pronounced swelling during processing.

The bulk of the SHP layer participates in forming the surface relief at low spatial frequencies. The combined action of the tension forces within the SHP layer and the surface tension forces produces a symmetric surface relief profile, yielding large values of h_{max} (about 1 μm), are comparable to the values of h_{max} for relief-phase holograms on SHP recorded in the setup with converging beams [3]. This scenario is shown schematically in Fig. 3,*c*, where the internal oblique-angled holographic structure is straightened on the surface and the relief acquires a quasi-sinusoidal character. The asymmetric relief characteristic for photoresists was obtained for SHP only on some samples with an ultra-low spatial frequency ($\nu < 40$ mm $^{-1}$) and is the exception rather than the rule. The height of the surface relief h at high spatial frequencies ($\nu > 500$ mm $^{-1}$), calculated from DE, tends to 0.22 μm, i.e., to the etching depth h_{etch}, characteristic for photoresists. This is due to the purely surface mechanism of relief formation associated with rapid absorption of short-wave UV radiation in gelatin and the short etching time, when the internal holographic structure is not affected by the last processing stages. However, in this case, unlike with photoresists, the surface relief for SHP becomes symmetric, most likely due to residual swelling of gelatin.

Thus, we established that including a stage when the photoemulsion is exposed to short-wave UV radiation into the processing procedure significantly expands the range of recorded spatial frequencies in which significant values of DE can be obtained for holographic transmission gratings. The achieved surface relief depths make it possible to produce highly efficient transmission-type relief-phase holographic structures in the region of low spatial frequencies. Holographic structures recorded in a setup with counter propagating beams can be effectively used in reflection after surface metallization at higher spatial frequencies.

REFERENCES

1. **Denisyuk Yu. N.,** The manifestation of the optical properties of an object in the wave field of the radiation it scatters, Dokl. Akad. Nauk SSSR. 144 (6) (1962) 1275–1278 (in Russian).

2. **Smith H. M.,** Photographic relief images, J. Opt. Soc. Am. 58 (4) (1968) 533–539.

3. **Gulyaev S. N., Ratushnyi V. P.,** Properties of relief-phase holograms produced by processing photographic plates with short wavelength UV radiation and with two-stage bleaching, J. Opt. Technol. 70 (2) (2003) 105–108.

4. **Sheridon N. K.,** Production of blazed holograms, Appl. Phys. Lett. 12 (9) (1968) 316–318.

5. **Pavlycheva N. K.,** Diffraction gratings for spectral devices (Review), J. Opt. Technol. 89 (3) (2022) 142 –150.

6. **Calixto S., Piazza V., Garnica G.,** Surface profile studies of photoinduced gratings made with DCG films with optional papain development, Gels. 8 (2) (2022) 102.

7. **Arkhipov A. V., Ganzherli N. M., Gulyaev S. N., Maurer I. A.,** High-frequency relief-phase holographic gratings on gelatin containing photosensitive media, J. Opt. Technol. 90 (3) (2023) 125–130.

8. **Moreau W. M.,** Positive photoresists, In book: W. M. Moreau, "Semiconductor lithography: Principles, practices and materials" (Part of the book series: "Microdevices (MDPF)"), Springer, New York, USA (1988) 29–34.

9. **Gulyaev S. N., Ganzherli N. M., Ilyushina D. A., Maurer I. A.,** Influence of ultraviolet irradiation on the formation of surface holographic structures recorded in a counter-directional recording scheme on photoemulsion layers, Proc. 2024 Int. Conf. on Electrical Engineering and Photonics (EExPolytech), Oct. 17–18, 2024. St. Petersburg, Russia. (2024) 454–456.

10. **Ganzherli N. M., Gulyaev S. N., Ilyushina D. A., Maurer I. A.,** Recording scheme in counterbeams for obtaining relief-phase holographic gratings working in transmission, Opt. Spectrosc. 132 (9) (2024) 908–910.

11. **Gulyaev S. N.,** Formation of the surface relief of holographic structures obtained by exposing photoemulsion to short-wave UV radiation, Nauchno-tekhnicheskie vedomosti SPbGPU. (3 (59)) (2008) 105–114 (in Russian).

12. **Ganzherli N. M., Gulyaev S. N., Maurer I. A.,** Improvement of the technology for manufacturing relief holographic gratings on dichromated gelatin irradiated with short-wave UV radiation, Opt. Spectrosc. 130 (13) (2022) 2011–2013.

СПИСОК ЛИТЕРАТУРЫ

1. **Денисюк Ю. Н.** Об отображении оптических свойств объекта в волновом поле рассеянного им излучения // Доклады Академии наук СССР. 1962. Т. 144. № 6. С. 1275–1278.

2. **Smith H. M.** Photographic relief images // Journal of the Optical Society of America. 1968. Vol. 58. No. 4. Pp. 533–539.

3. **Гуляев С. Н., Ратушный В. П.** Свойства рельефно-фазовых голограмм, полученных при обработке фотопластинок коротковолновым ультрафиолетовым излучением и двухступенчатом отбеливании // Оптический журнал. 2003. Т. 70. № 2. С. 45–49.

4. **Sheridon N. K.** Production of blazed holograms // Applied Physics Letters. 1968. Vol. 12. No. 9. Pp. 316–318.

5. **Павлычева Н. К.** Дифракционные решетки для спектральных приборов. Обзор // Оптический журнал. 2022. Т. 89. № 3. С. 28–41.

6. **Calixto S., Piazza V., Garnica G.** Surface profile studies of photoinduced gratings made with DCG films with optional papain development // Gels. 2022. Vol. 8. No. 2. P. 102.

7. **Архипов А. В., Ганжерли Н. М., Гуляев С. Н., Маурер И. А.** Рельефно-фазовые высокочастотные голографические решетки на содержащих желатин светочувствительных слоях // Оптический журнал. 2023. Т. 3 № .90. С. 47–38.

8. **Моро У.** Микролитография. В двух частях. Пер. с англ. М.: Мир, 1990. Часть 1 – 605 с. Часть 2 – 632 с.

9. **Gulyaev S. N., Ganzherli N. M., Ilyushina D. A., Maurer I. A.** Influence of ultraviolet irradiation on the formation of surface holographic structures recorded in a counter-directional recording scheme on photoemulsion layers // Proceedings of 2024 International Conference on Electrical Engineering and Photonics (EExPolytech). October 17–18, 2024. Saint Petersburg, Russia. Pp. 454–456.

10. **Ганжерли Н. М., Гуляев С. Н., Ильюшина Д. А., Маурер И. А.** Схема записи во встречных пучках для получения рельефно-фазовых голографических решеток, работающих на пропускание // Оптика и спектроскопия. 2024. Т. 132. № 9. С. 908–910.

11. **Гуляев С. Н.** Формирование поверхностного рельефа голографических структур, полученных при воздействии коротковолнового УФ-излучения на фотоэмульсию // Научно-технические ведомости СПбГПУ. Основной выпуск. 59) 3 № .2008). С. 114–105.

12. **Ганжерли Н. М., Гуляев С. Н., Маурер И. А.** Совершенствование технологии изготовления рельефных голографических решеток на бихромированном желатине, облученных коротковолновым УФ-излучением // Оптика и спектроскопия. 2021. Т. 129. № 10. С. 1276–1279.

THE AUTHORS

GULYAEV Sergey N.
Peter the Great St. Petersburg Polytechnic University
29 Politechnicheskaya St., St. Petersburg, 195251, Russia
SGulyaev@spbstu.ru
ORCID: 0000-0003-0549-0961

GANZHERLI Nina M.
Ioffe Institute of RAS
26 Polytekhnicheskaya St., St. Petersburg, 194021, Russia
nina.holo@mail.ioffe.ru
ORCID: 0000-0002-2933-2135

ILYUSHINA Darina A.
Peter the Great St. Petersburg Polytechnic University
29 Politechnicheskaya St., St. Petersburg, 195251, Russia
ilyushina.da@edu.spbstu.ru

MAURER Irina A.
Ioffe Institute of RAS
26 Polytekhnicheskaya St., St. Petersburg, 194021, Russia
maureririna@yandex.ru
ORCID: 0000-0001-9385-4221

СВЕДЕНИЯ ОБ АВТОРАХ

ГУЛЯЕВ Сергей Николаевич – *кандидат физико-математических наук, ведущий инженер Высшей инженерно-физической школы Санкт-Петербургского политехнического университета Петра Великого.*
195251, Россия, г. Санкт-Петербург, Политехническая ул., 29
SGulyaev@spbstu.ru
ORCID: 0000-0003-0549-0961

ГАНЖЕРЛИ Нина Мануиловна – *кандидат физико-математических наук, старший научный сотрудник Физико-технического института имени А. Ф. Иоффе РАН.*
194021, Россия, г. Санкт-Петербург, Политехническая ул., 26
nina.holo@mail.ioffe.ru
ORCID: 0000-0002-2933-2135

ИЛЬЮШИНА Дарина Алексеевна – *студентка Института электроники и телекоммуникаций Санкт-Петербургского политехнического университета Петра Великого.*
195251, Россия, г. Санкт-Петербург, Политехническая ул., 29
ilyushina.da@edu.spbstu.ru

МАУРЕР Ирина Анатольевна – *кандидат технических наук, старший научный сотрудник Физико-технического института имени А. Ф. Иоффе РАН.*
194021, Россия, г. Санкт-Петербург, Политехническая ул., 26
maureririna@yandex.ru
ORCID: 0000-0001-9385-4221

Received 23.05.2025. Approved after reviewing 10.06.2025. Accepted 10.06.2025.
Статья поступила в редакцию 23.05.2025. Одобрена после рецензирования 10.06.2025. Принята 10.06.2025.